Asian Journal of Chemistry; Vol. 36, No. 12 (2024), 2755-2759

ASIAN JOURNAL OF CHEMISTRY

https://doi.org/10.14233/ajchem.2024.31962

Photocatalytic Degradation of Tetracycline Hydrochloride using Hybrid C_{60} Fullerene Nanowhisker-Zeolitic Imidazolate Framework-8 Composite under Blue Light Emitting Diode Irradiation

S.W. Ko and H. Chung*

Department of Convergence Science, Graduate School, Sahmyook University, 815, Seoul 139-742, Republic of Korea

*Corresponding author: Tel: +82 2 33991754; E-mail: larus@nate.com

Received: 16 May 2024; *Accepted*: 29 June 2024; *Published online*: 30 November 2024; AJC-21814

The C_{60} fullerene nanowhisker (FNW)-zeolitic imidazolate framework-8 (ZIF-8) composite was synthesized using C_{60} fullerene nanowhisker, 2-methyl imidazole, zinc nitrate hexahydrate in methanol. The characterization of C_{60} FNW-ZIF-8 composite was identified using X-ray diffraction (XRD), Raman spectroscopy and scanning electron microscopy (SEM). The photocatalytic activity for tetracycline hydrochloride degradation was confirmed by UV-visible spectroscopy. A kinetic study indicated that hybrid nanocomposite catalyzed the photodegradation of tetracycline hydrochloride under blue light emitting diode (LED) irradiation following a pseudo-first-order reaction rate law.

Keywords: C_{60} fullerene nanowhisker, Imidazolate framework-8, Photocatalytic activity, Tetracycline, Light emitting diode.

INTRODUCTION

Tetracycline hydrochloride (TC) is a widely recognized antibiotic and plays a crucial role in the prevention and treatment of bacterial infections in both humans and animals [1,2]. Common antibiotics like tetracycline hydrochloride have great hydrophilicity and structural stability; so, they cannot be readily broken down or eliminated by traditional sewage treatment plants. Therefore, the prolonged accumulation of tetracycline hydrochloride in ecosystems has resulted in significant adverse impacts on both the ecological environment and human health [3,4]. Hence, the elimination of tetracycline from the environment is essential for the sustainability of environment and human health [2]. Various techniques have been explored to remove tetracycline from the aqueous solutions, *e.g.* ion-exchange, nanofiltration, adsorption, semiconductor photocatalysis and others [2,5-14]. Among these techniques, photocatalysis stands out as a popular process and has been extensively studied using various semi-conductor catalysts [2,15-18].

C_{60} fullerene discovered in 1985, has garnered considerable attention due to its unique structure and properties [19]. In 2001, Miyazawa *et al*. [20] discovered fine crystalline fibers composed of C_{60} fullerene, termed C_{60} fullerene nanowhiskers (FNWs), using a lead zirconate titanate colloidal solution containing C_{60} fullerene. These C_{60} FNWs used as supports for immobilizing active catalytic materials [21,22]. These materials have been utilized in a wide range of applications, such as catalysis and photocatalysis, and have the capability of functioning as a semi-conducting material [23].

The C_{60} fullerene nanowhiskers (FNWs) were prepared using the liquid-liquid interfacial precipitation method and exhibited unique properties such as high charge carrier mobility, optical transmittance than that of pristine C_{60} fullerene [24-27]. Owing to these unique properties, C_{60} FNWs serve as excellent electron acceptors and transport materials in hybrid C_{60} FNWs based composites.

A novel class of crystalline and microporous material, known as zeolitic imidazolate framework (ZIF), has been rapidly proliferating owing to its significant potential in diverse applications, including gas adsorption, molecular separation, chemical sensing [28], catalysis [29-32] and water purification [33,34]. ZIF possesses a three-dimensional pore network created by the coordination of metal and imidazolate ions in a tetrahedral arrangement [35]. The advantage of ZIF compared to other inorganic materials is its structural flexibility, which is influenced by the diverse selection of metals and imidazole used in its synthesis [35]. ZIF-8 is distinguished as one of the most extensively studied the ZIF structures, owing to its remark-

able stability in response to temperature fluctuations and chemical reactions [35]. Furthermore, its extensive interior surface area contributes to its efficacy in many applications [35-37].

In this study, a new type of hybrid C_{60} FNW-ZIF-8 composite is fabricated to use a photocatalyst to degrade tetracycline hydrochloride antibiotic under blue LED irradiation. Also, the photocatalytic activity and kinetic study were also evaluated for the degradation of tetracycline antibiotic using hybrid C_{60} FNW-ZIF-8 composite under blue LED irradiation at 450 nm, employing UV-vis spectrophotometry.

EXPERIMENTAL

Toluene and 2-propanol were purchased from Dajung Chemicals, Korea. Tetracycline hydrochloride ($C_{22}H_{24}N_2O_8$·HCl) and sodium borohydride ($NaBH_4$) were provided by Sigma-Aldrich, USA. The C_{60} fullerene, zinc nitrate hexahydrate [$Zn(NO_3)_2$·$6H_2O$] and 2-methylimidazole were obtained from Alfa Aesar, USA. Powder X-ray diffraction (XRD; D8 Advance, Bruker, Germany) was used to investigate the crystal structure of the hybrid nanocomposites. Cu K_α radiation (λ = 0.154178 nm) was used at 40 kV and 40 mA in a 2θ range of 5º to 90º, with a scan speed of 0.2 s/step and a step size of 0.02º. Raman spectroscopy (B&W Tek i-Raman Plus instrument, BWS465-532S, USA) was used to examine the lattice vibrations of the samples with the spectrum excited with 532 nm radiation from a 40 mW Nd:YAG laser. The surfaces of hybrid nanocomposite were examined using scanning electron microscopy (JSM-6510, JEOL Ltd., Japan) at a magnification of 5500X, 15000X and an accelerating voltage of 10-40 kV. UV-vis spectrophotometry (Shimadzu UV-1691 PC) was used to evaluate the photocatalytic activity and to study the kinetics of the synthesized C_{60} FNW-ZIF-8 composite for the degradation of tetracycline under LED irradiation at 450 nm. LED lamp (10W, 450 nm, LED T5 Jinsung Electronic., Ltd., China) was served as light source.

Synthesis of ZIF-8 nanoparticles: In brief, 2.97 mmol of $Zn(NO_3)_2$·$6H_2O$ and 12.00 mmol of 2-methylimidazole were dissolved in 40 mL of methanol with stirring for 20 min and left to stand for 24 h. The resulting product was separated by centrifugation, thoroughly washed with methanol to remove any remaining raw materials and then dried at 50 ºC for 2 h.

Synthesis of C_{60} FNWs: The liquid-liquid interfacial precipitation (LLIP) method was used to synthesize C_{60} FNWs by mixing isopropyl alcohol with C_{60}-saturated toluene in a volume ratio of 5:1. After obtaining the mixture solution, it was stored at 5 ºC for 72 h. Subsequently, the precipitate was centrifuged and dried in an oven at 60 ºC for 5 h to obtain a solid powder sample.

Synthesis of C_{60} FNW–ZIF-8 composite: The synthesized C_{60} FNWs (250 mg) were dispersed in 25 mL of methanol and stirred for 5 min. The resulting C_{60} FNWs solution was then combined with 25 mL of a methanol solution containing zinc nitrate hexahydrate ($Zn(NO_3)_2$·$6H_2O$, 0.725 g) and 25 mL of a methanol solution containing 2-methylimidazole ($C_4H_6N_2$, 0.41 g). After stirring for 5 h, the mixture solution was left to stand for 22 h. The resulting precipitate was repeatedly washed with methanol and dried in an oven at 60 ºC for 2 h to obtain a powder sample.

Photocatalytic activity and kinetics study: The photocatalytic activities of both the ZIF-8 nanoparticles and C_{60} FNW-ZIF-8 composite materials for the degradation of tetracycline in aqueous solution were evaluated using a blue LED at 450 nm as light source at room temperature. First, 0.5 mg/mL of photocatalyst was added to 10 mL solution of tetracycline hydrochloride (0.1 mg/mL) and the conical tubes were then kept in darkness for 15 min. The absorption peak of TC was measured using UV-vis spectroscopy (Shimadzu UV-1691 PC) in the wavelength range of 356~380 nm at 15 min intervals.

RESULTS AND DISCUSSION

XRD studies: The XRD patterns (Fig. 1) depict the crystal structure of ZIF-8 nanoparticles (a) and C_{60} FNW-ZIF-8 composite (b). In Fig. 1a, the peaks observed at 2θ = 7.56º, 10.46º, 12.72º, 14.89º, 16.54º, 18.22º, 22.23º, 23.47º, 26.70º and 29.72º correspond to the (011), (022), (112), (022), (013), (222), (144), (233), (044) and (244) planes, respectively, indicating the ZIF-8 structure [38,39]. In Fig. 1b, the peaks at 2θ = 10.81º, 17.64º, 20.62º and 28.32º in the powder XRD pattern correspond to the (111), (220), (311) and (422) planes of the C_{60} fullerene nanowhisker, respectively [22]. Furthermore, the XRD data showed that the C_{60} FNW–ZIF-8 composite was successfully synthesized. Additionally, the mean crystallite size of ZIF-8 particles was calculated using Scherrer's formula [$D = k\lambda/\beta\cos\theta$], where D is the crystallite size, λ is the wavelength of the CuK_α radiation (λ = 0.154178 nm), k is a shape factor (taken as 0.94), 2θ is the angle between the incident and scattered X-rays and β is the full width at half maximum (FWHM). The average crystallite size of ZIF-8 nanoparticles was determined to be approximately 29.83 nm (Table-1).

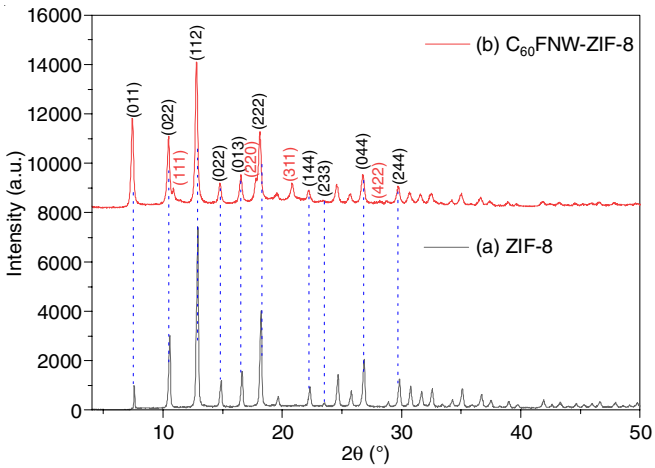

Fig. 1. XRD patterns of (a) ZIF-8 nanoparticle and (b) C_{60} FNW-ZIF-8 composite

TABLE-1
DETAILS OF CRYSTALLITE SIZE OF ZIF-8 IN C_{60} FNW–ZIF-8 COMPOSITE

Peak	Plane (*hkl*)	2θ (°)	FWHM (°)	Crystallite size (nm)
ZIF-8	112	12.72	0.28	29.83

Raman spectral studies: Fig. 2 shows the Raman spectra of ZIF-8 nanoparticles and C_{60} FNW-ZIF-8 composite. The Raman shift of C_{60} FNW-ZIF-8 composite indicated Hg (1) at 268 cm^{-1}, Ag (1) at 489 cm^{-1} and Ag (2) at 1458 cm^{-1} due to the C_{60} FNW [40]. Furthermore, the bands at 180 cm^{-1} and 1146 cm^{-1} may be correspond to the Zn-N and C-N stretching vibrations of ZIF-8 nanoparticles [41,42].

SEM studies: Fig. 3 shows SEM images of ZIF-8 nanoparticles and C_{60} FNW-ZIF-8 composite. ZIF-8 nanoparticles appeared cubic shape in Fig. 3a, whereas cubic shaped ZIF-8 was placed on the needle-like structure of C_{60} fullerene nanowhisker (Fig. 3b).

Photocatalytic activity and kinetic study: Fig. 4 presents UV-vis spectra for photocatalytic degradation of tetracycline hydrochloride (TC) using C_{60} FNW–ZIF-8 composite and ZIF-8 nanoparticle. The percent of degradation of tetracycline hydrochloride was calculated using the following eqn. 1 [43]:

$$TC = \left(\frac{C_0 - C}{C_0}\right) \times 100\% \quad (1)$$

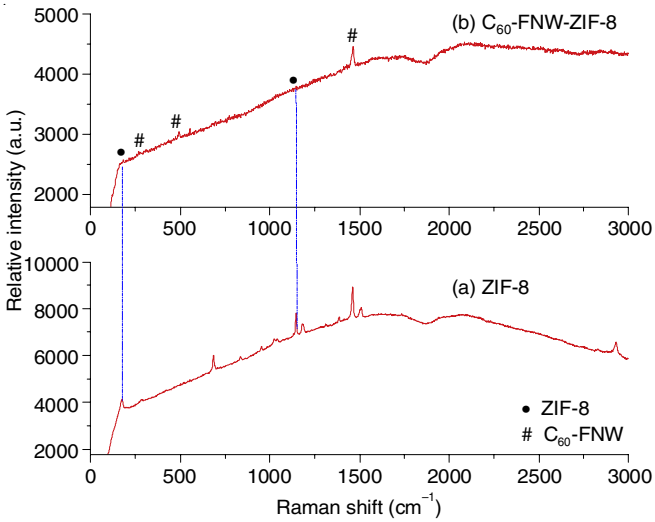

Fig. 2. Raman spectra of (a) ZIF-8 nanoparticle and (b) C_{60} FNW-ZIF-8 composite

where C_0 is the initial concentration of tetracycline hydrochloride after adsorption for 15 min; and C is the concentration

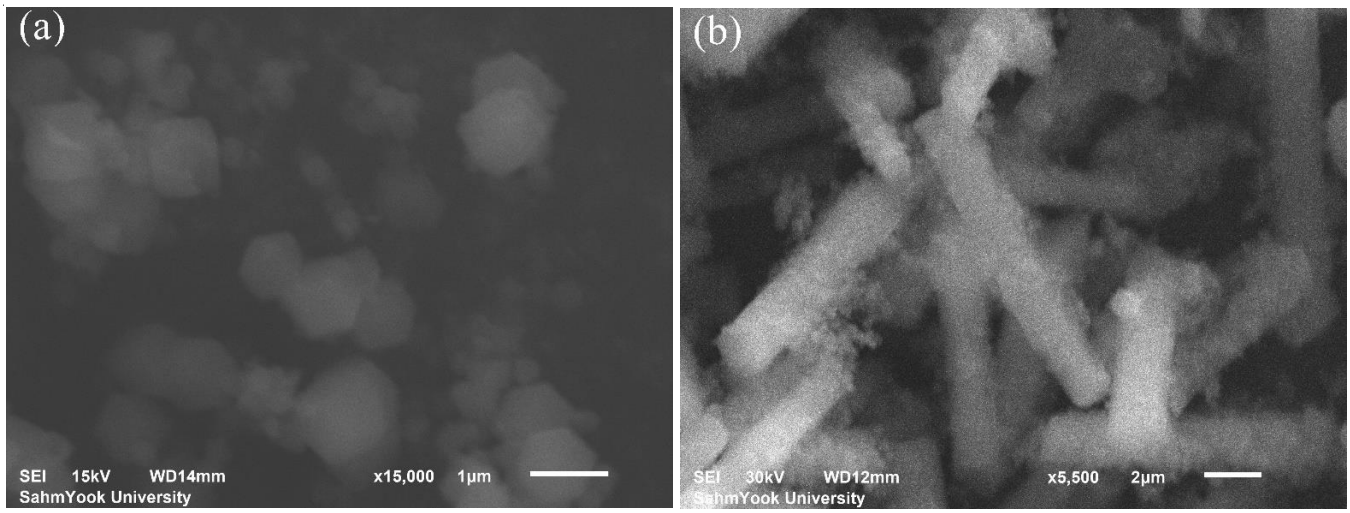

Fig. 3. SEM images of (a) ZIF-8 nanoparticle and (b) C_{60} FNW-ZIF-8 composite

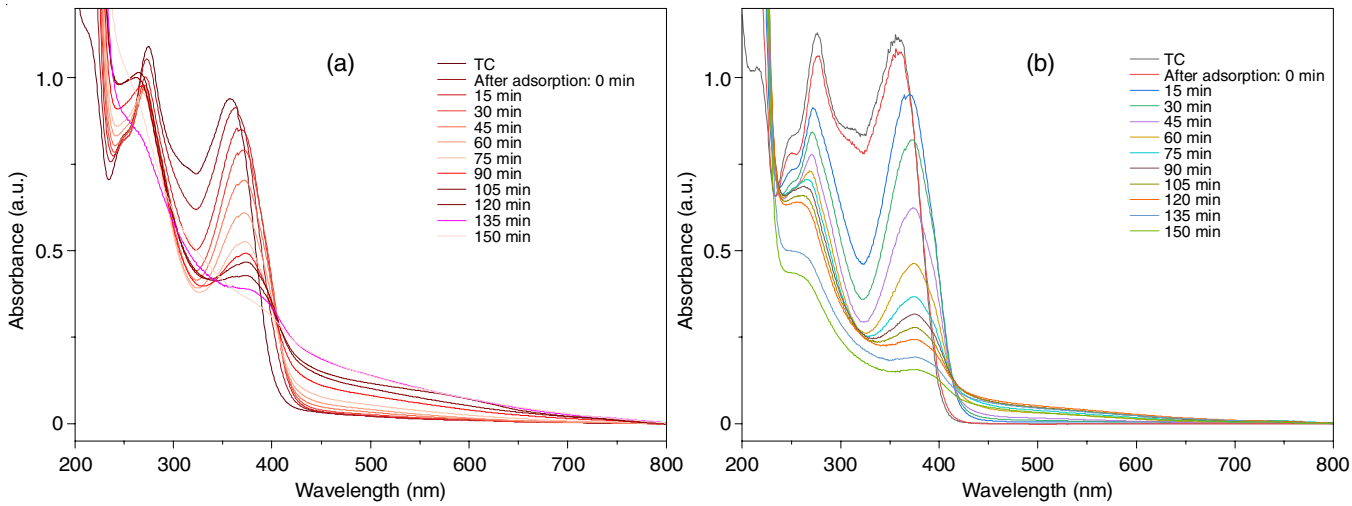

Fig. 4. UV-vis spectra of photocatalytic degradation of tetracycline hydrochloride using (a) ZIF-8 nanoparticle and (b) C_{60} FNW-ZIF-8 composite under blue LED irradiation at 450 nm

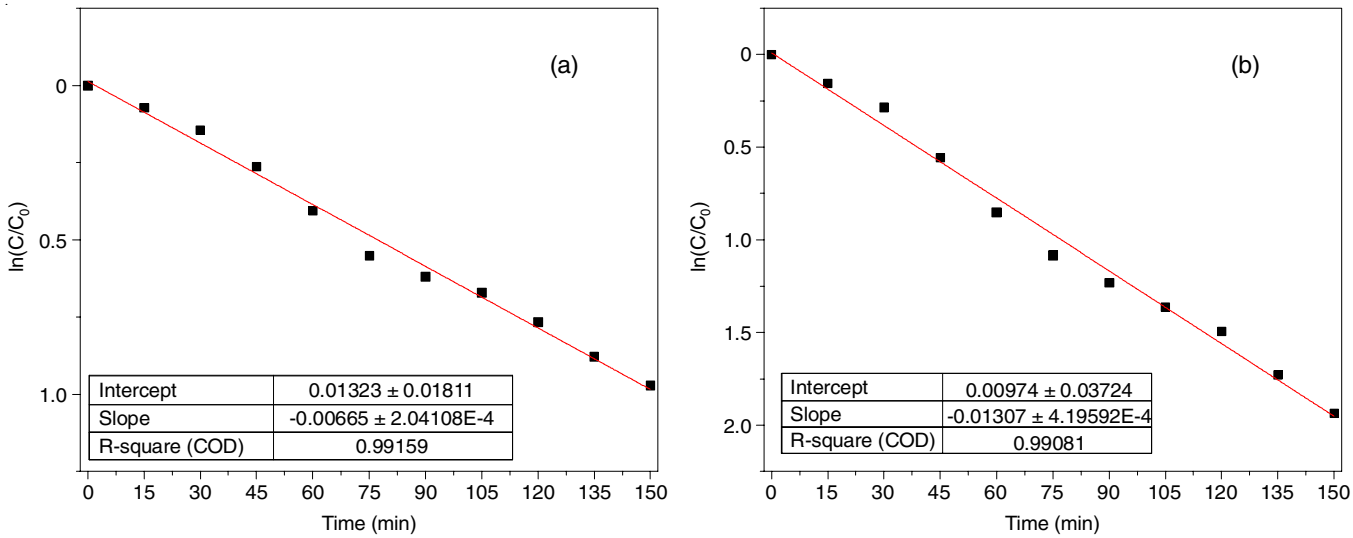

Fig. 5. Kinetics study for degradation of tetracycline hydrochloride under blue LED irradiation at 450 nm using (a) ZIF-8 nanoparticle and (b) C_{60} FNW-ZIF-8 composite as photocatalysts

of tetracycline hydrochloride at time t. Both C_0 and C values were determined from the maximum absorption observed in the UV-vis absorption spectra in the range of 356~380 nm. The degradation percentage of tetracycline hydrochloride, when utilizing ZIF-8 nanoparticle as a photocatalyst, was found to be 56.79% under blue LED irradiation at 450 nm for 150 min (Fig. 4a). Furthermore, Fig. 4b shows that 92.77% of tetracycline hydrochloride was degraded when employing the C_{60} FNW-ZIF-8 composite as a photocatalyst under the same conditions. Fig. 5 presents the results of the kinetics study for the photocatalytic degradation of tetracycline hydrochloride using C_{60} FNW–ZIF-8 composite and ZIF-8 nanoparticle under blue LED irradiation at 450 nm. The first-order reaction is represented by eqn. 2:

$$\ln\left(\frac{C}{C_0}\right) = -k_1 C \quad (2)$$

where k_1 is the rate constant; C_0 is the starting concentration of tetracycline hydrochloride; and C is the concentration at time t. The photocatalytic degradation of tetracycline hydrochloride over the photocatalysts in Fig. 5 is demonstrated by the linear behaviour of the slopes, which follows pseudo-first-order kinetics. The R^2 values (coefficient of determination) for the pseudo-first-order reaction kinetics were 0.992 in Fig. 5a and 0.991 in Fig. 5b.

Conclusion

In this work, a novel hybrid C_{60} fullerene nanowhisker (FNW)-zeolitic imidazolate framework-8 (ZIF-8) composite was synthesized using zinc nitrate hexahydrate, 2-methyl imidazole and C_{60} fullerene nanowhisker. The characterization of C_{60} FNW-ZIF-8 composite was affirmed using XRD, Raman spectroscopy and SEM techniques. The photocatalytic degradation of tetracycline hydrochloride under blue LED irradiation (at 450 nm) was carried out using ZIF-8 nanoparticle and C_{60} FNW-ZIF-8 composite. Overall, compared to ZIF-8 alone, the C_{60} FNW-ZIF-8 composite demonstrated improved photocatalytic degradation activity for tetracycline hydrochloride. Furthermore, kinetics analysis of the photocatalytic degradation of tetracycline hydrochloride using both ZIF-8 nanoparticles and C_{60} FNW-ZIF-8 composite as catalysts revealed a pseudo-first-order reaction rate law.

ACKNOWLEDGEMENTS

This study was supported by research funding from Sahmyook University in Korea.

CONFLICT OF INTEREST

The authors declare that there is no conflict of interests regarding the publication of this article.

REFERENCES

1. M.B. Ahmed, J.L. Zhou, N.H. Ngo and W. Guo, *Sci. Total Environ.*, **532**, 112 (2015); https://doi.org/10.1016/j.scitotenv.2015.05.130
2. S. Wu, H. Hu, Y. Lin, J. Zhang and Y.H. Hu, *Chem. Eng. J.*, **382**, 122842 (2020); https://doi.org/10.1016/j.cej.2019.122842
3. X.W. Zhang, F. Wang, C.C. Wang, P. Wang, H. Fu and C. Zhao, *Chem. Eng. J.*, **426**, 131927 (2021); https://doi.org/10.1016/j.cej.2021.131927
4. Y. Zhao, Y. Li, L. Chang, W. He, K. Liu, M. Cui, S. Wang, Y. Zhao and X. Tan, *RSC Adv.*, **14**, 4861 (2024); https://doi.org/10.1039/D3RA08225C
5. P. Zhang, Y. Li, Y. Cao and L. Han, *Bioresour. Technol.*, **285**, 121348 (2019); https://doi.org/10.1016/j.biortech.2019.121348
6. I.C. Iakovides, I. Michael-Kordatou, N.F.F. Moreira, A.R. Ribeiro, T. Fernandes, M.F.R. Pereira, O.C. Nunes, C.M. Manaia, A.M.T. Silva and D. Fatta-Kassinos, *Water Res.*, **159**, 333 (2019); https://doi.org/10.1016/j.watres.2019.05.025
7. A.M. Cahino, M.M.A. de Andrade, E.S. de Araújo, E.L. Silva, C.D.O. Cunha and E.M.R. Rocha, *Environ. Qual. Manage.*, **28**, 101 (2018); https://doi.org/10.1002/tqem.21579
8. J. Wang, D. Zhi, H. Zhou, X. He and D. Zhang, *Water Res.*, **137**, 324 (2018); https://doi.org/10.1016/j.watres.2018.03.030

9. X. Wen, Z. Zeng, C. Du, D. Huang, G. Zeng, R. Xiao, C. Lai, P. Xu, C. Zhang, J. Wan, L. Hu, L. Yin, C. Zhou and R. Deng, *Chemosphere*, **222**, 865 (2019); https://doi.org/10.1016/j.chemosphere.2019.02.020
10. G.H. Yang, D.D. Bao, D.Q. Zhang, C. Wang, L.L. Qu and H.T. Li, *Nanoscale Res. Lett.*, **13**, 146 (2018); https://doi.org/10.1186/s11671-018-2555-9
11. J. Hou, Z. Chen, J. Gao, Y. Xie, L. Li, S. Qin, Q. Wang, D. Mao and Y. Luo, *Water Res.*, **159**, 511 (2019); https://doi.org/10.1016/j.watres.2019.05.034
12. H. Wang, Y. Wu, M. Feng, W. Tu, T. Xiao, T. Xiong, H. Ang, X. Yuan and J.W. Chew, *Water Res.*, **144**, 215 (2018); https://doi.org/10.1016/j.watres.2018.07.025
13. I.A. Vasiliadou, R. Molina, M.I. Pariente, K.C. Christoforidis, F. Martinez and J.A. Melero, *Chem. Eng. J.*, **359**, 1427 (2019); https://doi.org/10.1016/j.cej.2018.11.035
14. H. Xiong, S. Dong, J. Zhang, D. Zhou and B.E. Rittmann, *Water Res.*, **136**, 75 (2018); https://doi.org/10.1016/j.watres.2018.02.061
15. A. Truppi, F. Petronella, T. Placido, V. Margiotta, G. Lasorella, L. Giotta, C. Giannini, T. Sibillano, S. Murgolo, G. Mascolo, A. Agostiano, M.L. Curri and R. Comparelli, *Appl. Catal. B*, **243**, 604 (2019); https://doi.org/10.1016/j.apcatb.2018.11.002
16. L. Chen, S. Yang, Y. Huang, B. Zhang, F. Kang, D. Ding and T. Cai, *J. Hazard. Mater.*, **371**, 566 (2019); https://doi.org/10.1016/j.jhazmat.2019.03.038
17. J. Lyu, J. Shao, Y. Wang, Y. Qiu, J. Li, T. Li, Y. Peng and F. Liu, *Chem. Eng. J.*, **358**, 614 (2019); https://doi.org/10.1016/j.cej.2018.10.085
18. L. Rimoldi, D. Meroni, G. Cappelletti and S. Ardizzone, *Catal. Today*, **281**, 38 (2017); https://doi.org/10.1016/j.cattod.2016.08.015
19. L.K. Shrestha, R.G. Shrestha, J.P. Hill and K. Ariga, *J. Oleo Sci.*, **62**, 541 (2013); https://doi.org/10.5650/jos.62.541
20. K. Miyazawa, A. Obayashi and M. Kuwabara, *J. Am. Ceram. Soc.*, **84**, 3037 (2001); https://doi.org/10.1111/j.1151-2916.2001.tb01133.x
21. J.W. Ko, S. Jeon and W.B. Ko, *Fuller. Nanotub. Carbon Nanostruct.*, **28**, 642 (2020); https://doi.org/10.1080/1536383X.2020.1733533
22. J.W. Ko, S.H. Park, S. Jeon, H. Chung and W.B. Ko, *Fuller. Nanotub. Carbon Nanostruct.*, **30**, 584 (2022); https://doi.org/10.1080/1536383X.2021.1978985
23. K. Miyazawa, M. Yoshitake and Y. Tanaka, *Surf. Eng.*, **34**, 846 (2018); https://doi.org/10.1080/02670844.2017.1396779
24. B.H. Cho, K.B. Lee, K. Miyazawa and W.B. Ko, *Asian J. Chem.*, **25**, 8027 (2013); https://doi.org/10.14233/ajchem.2013.14974
25. K. Miyazawa, *Sci. Technol. Adv. Mater.*, **16**, 013502 (2015); https://doi.org/10.1088/1468-6996/16/1/013502
26. R. Kato and K. Miyazawa, *J. Nanotechnol.*, **2012**, 101243 (2012); https://doi.org/10.1155/2012/101243
27. J.W. Ko, Y.A. Son and W.B. Ko, *Elastom. Compos.*, **55**, 321 (2020); https://doi.org/10.7473/EC.2020.55.4.321
28. R. Ameloot, E. Gobechiya, H. Uji-i, J.A. Martens, J. Hofkens, L. Alaerts, B.F. Sels and D.E. De Vos, *Adv. Mater.*, **22**, 2685 (2010); https://doi.org/10.1002/adma.200903867
29. Y. Pan, Y. Liu, G. Zeng, L. Zhao and Z. Lai, *Chem. Commun.*, **47**, 2071 (2011); https://doi.org/10.1039/c0cc05002d
30. M. Zhu, S.R. Venna, J.B. Jasinski and M.A. Carreon, *Chem. Mater.*, **23**, 3590 (2011); https://doi.org/10.1021/cm201701f
31. S. Tanaka, K. Kida, M. Okita, Y. Ito and Y. Miyake, *Chem. Lett.*, **41**, 1337 (2012); https://doi.org/10.1246/cl.2012.1337
32. A. Phan, C.J. Doonan, F.J. Uribe-Romo, C.B. Knobler, M. O'keeffe and O.M. Yaghi, *Acc. Chem. Res.*, **43**, 58 (2010); https://doi.org/10.1021/ar900116g
33. J. Duan, Y. Pan, F. Pacheco, E. Litwiller, Z. Lai and I. Pinnau, *J. Membr. Sci.*, **476**, 303 (2015); https://doi.org/10.1016/j.memsci.2014.11.038
34. L. Wang, M. Fang, J. Liu, J. He, L. Deng, J. Li and J. Lei, *RSC Adv.*, **5**, 50942 (2015); https://doi.org/10.1039/C5RA06185G
35. J.J. Beh, J.K. Lim, E.P. Ng and B.S. Ooi, *Mater. Chem. Phys.*, **216**, 393 (2018); https://doi.org/10.1016/j.matchemphys.2018.06.022
36. J. Cravillon, S. Münzer, S.J. Lohmeier, A. Feldhoff, K. Huber and M. Wiebcke, *Chem. Mater.*, **21**, 1410 (2009); https://doi.org/10.1021/cm900166h
37. K. Kida, M. Okita, K. Fujita, S. Tanaka and Y. Miyake, *CrystEngComm*, **15**, 1794 (2013); https://doi.org/10.1039/c2ce26847g
38. A. Schejn, L. Balan, V. Falk, L. Aranda, G. Medjahdi and R. Schneider, *CrystEngComm*, **16**, 4493 (2014); https://doi.org/10.1039/C3CE42485E
39. L.T.L. Nguyen, K.K.A. Le and N.T.S. Phan, *Chin. J. Catal.*, **33**, 688 (2012); https://doi.org/10.1016/S1872-2067(11)60368-9
40. J.W. Ko and W.B. Ko, *Mater. Trans.*, **57**, 2122 (2016); https://doi.org/10.2320/matertrans.M2016214
41. D. Radhakrishnan and C. Narayana, *J. Chem. Phys.*, **144**, 134704 (2016); https://doi.org/10.1063/1.4945013
42. G. Kumari, K. Jayaramulu, T.K. Maji and C. Narayana, *J. Phys. Chem. A*, **117**, 11006 (2013); https://doi.org/10.1021/jp407792a
43. T.A. Saleh and V.K. Gupta, *J. Colloid Interface Sci.*, **371**, 101 (2012); https://doi.org/10.1016/j.jcis.2011.12.038